DOE Award DE-FE0031548

High Temperature Electrochemical Sensors for In-situ Corrosion Monitoring In Coal-Based Power Generation Boilers

Xingbo Liu, Debangsu Bhattacharyya, Shanshan Hu, Tianliang Zhao, Liang Ma
West Virginia University

Brandon Rumberg
Aspinity

Jared Custer, Chad Hufnagel
Longview Power

LONGVIEW POWER LLC

ASPINITY

OUTLINE

- Technical Background
- Project Objectives
- Field Test Results
- Reference Electrode Development
- Corrosion Database Development
- Techno-Economical Analysis Progress
- Summary and Future Work
- Acknowledgement

Hot Corrosion Mechanism

Hot corrosion: the degradation of an alloy at elevated temperature induced by a thin molten salt layer under an oxidizing atmosphere.

O_2-SO_2-SO_3

Sulfate salt	Tm (°C)
Na_2SO_4	884
K_2SO_4	1069
Na_2SO_4-$CoSO_4$	575
K_2SO_4-$CoSO_4$	535
$K_3Fe(SO_4)_3$	624
$Na_3Fe(SO_4)_3$	618
$Na_2S_2O_7$	400.9
$K_2S_2O_7$	325

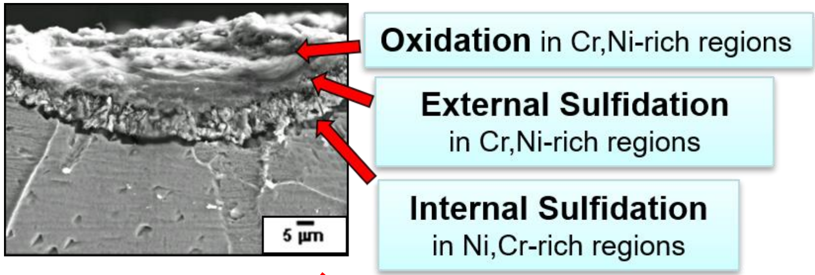

Metal oxide alkaline sulfate

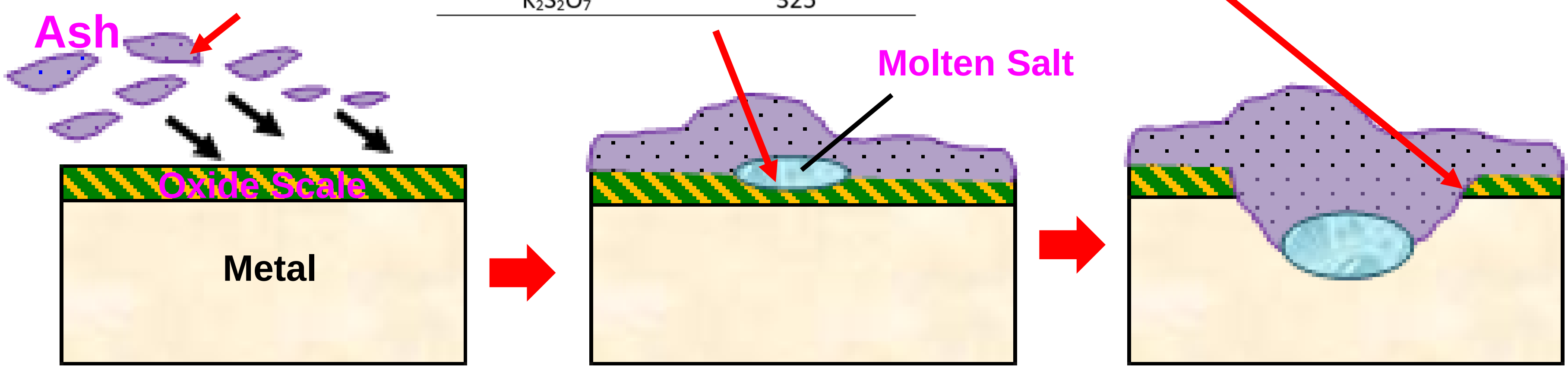

Ash deposition

Formation of molten salt and fluxing away of protective oxide film

Direct reaction between bare metal and reduced sulphate species

Schematic of hot corrosion mechanism induced by coal ash

Aung, Naing Naing, and **Xingbo Liu***. Corrosion science 76 (2013): 390-402.

Self-Powered Wireless-Ready Electrochemical Sensor For In-Situ Corrosion Monitoring of Coal-Fired A-USC Boiler Tubes

- DoE Award No. DE- FE0005717
- Funded by NETL – Coal Utilization Science Program (2010-2015)
- Team: WVU, Special Metals, International Zinc Association, Western Research Institute

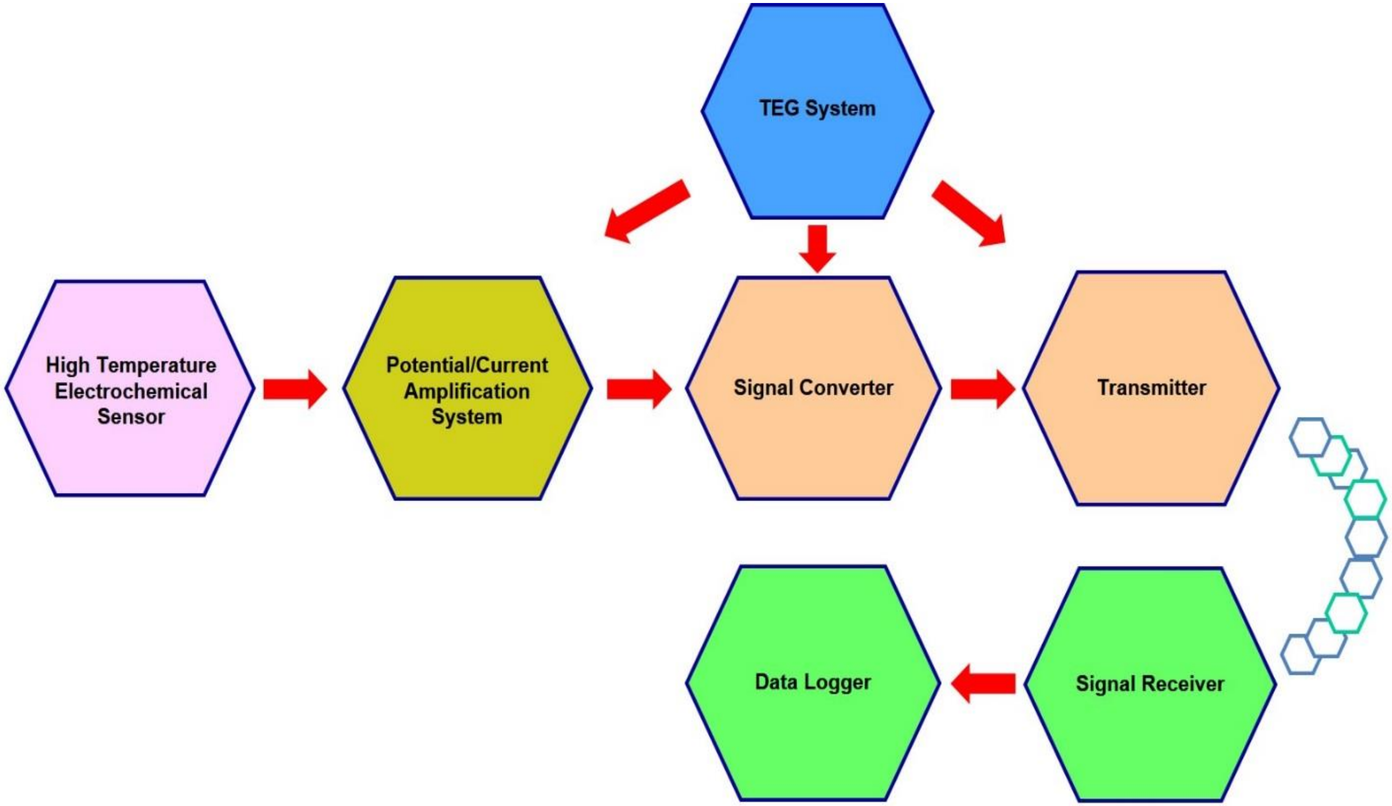

Conceptual design of the self-powered HT corrosion sensor system

Aung, Naing Naing, Edward Crowe, and **Xingbo Liu***. ISA transactions 55 (2015): 188-194.

Oxygen and Sulfur Diffusion During Oxidation & Sulfidation Stages

Two stages of hot corrosion were revealed by SEM: oxidation and sulfidation (external sulfidation and internal sulfidation).

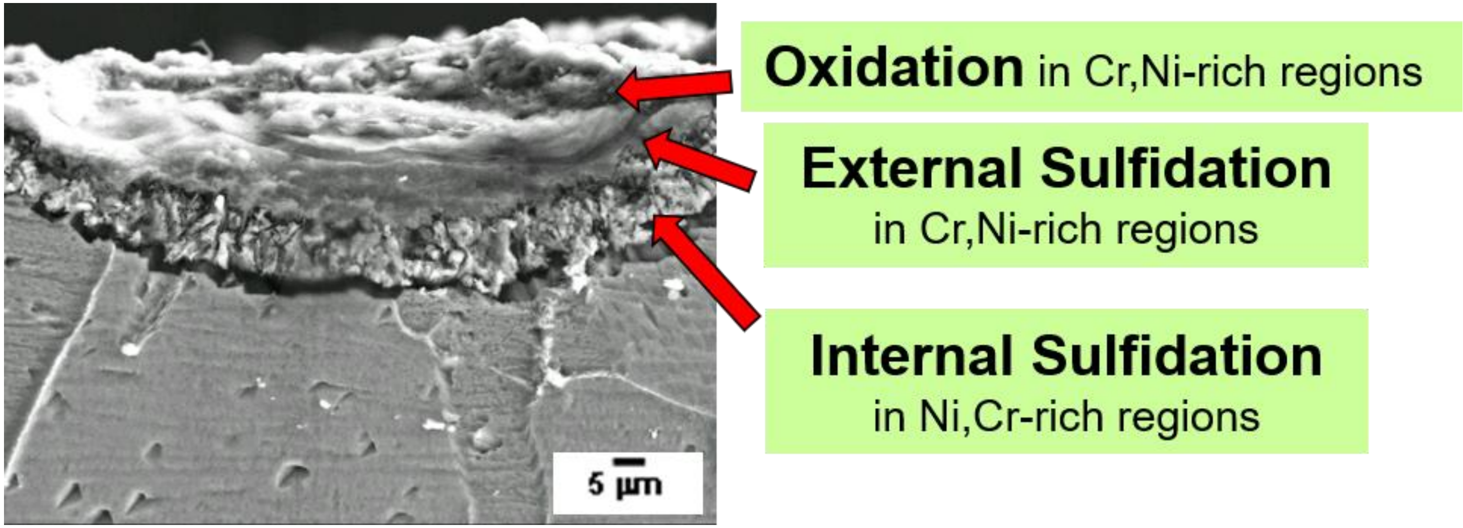

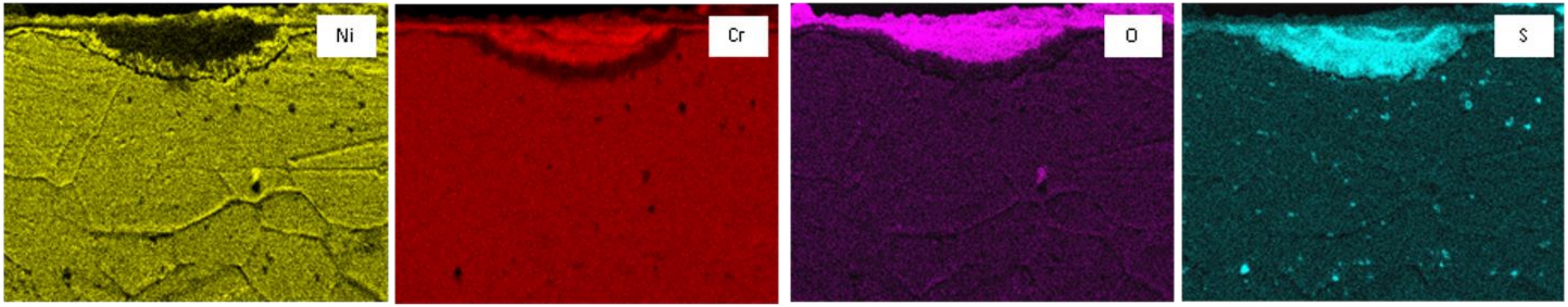

Morphology and element distribution of cross-sectional morphology of corroded sample

Aung, Naing Naing, and **Xingbo Liu***. Corrosion science 76 (2013): 390-402.
Aung, Naing Naing, and **Xingbo Liu*.** Corrosion science 82 (2014): 227-238.

Reproducibility of Potential and Current Signals During Oxidation and Sulfidation

Both potential and current noise are effective and efficient signals to reveal the stages of corrosion process (oxidation and sulfidation) in the simulated coal-fired power plant environment.

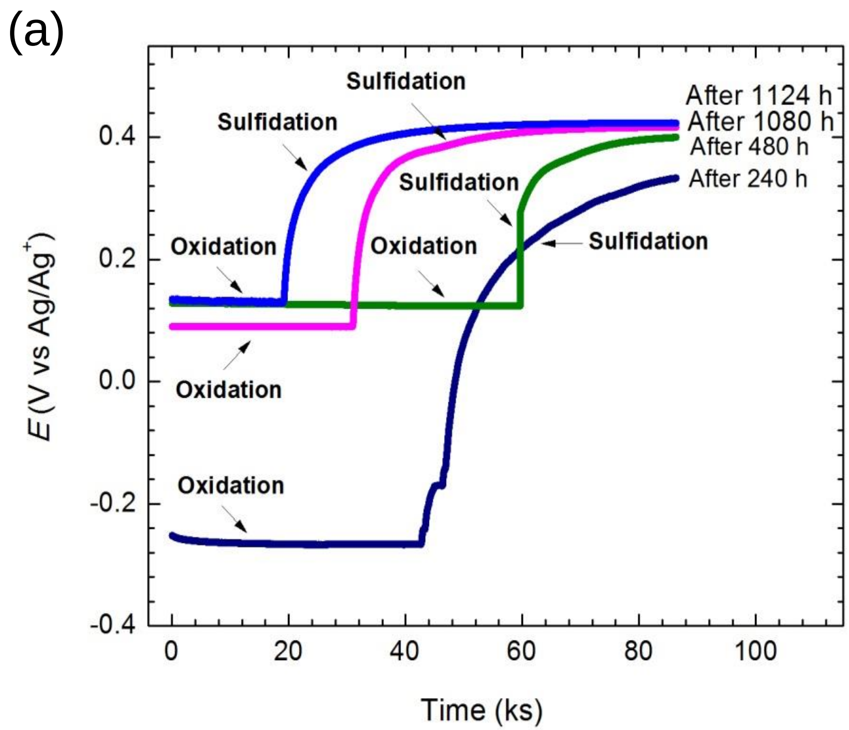

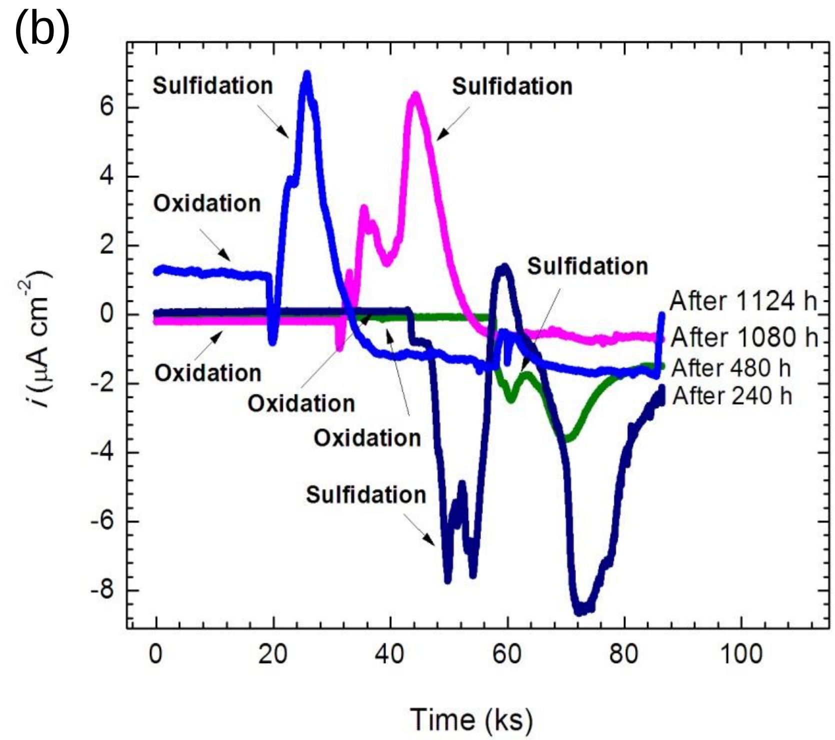

Fig.6 (a) potential and (b) current noise signals obtained for Inconel 740 alloy beneath a thin layer of coal ash at 850 ºC

Aung, Naing Naing, Edward Crowe, and **Xingbo Liu***. ISA transactions 55 (2015): 188-194.

FIVE Typical Noise Signals Measured in the Coal Ash Hot Corrosion Process

Electrochemical Potential Noise Signals

- The noise signature of a gradual potential continuously changing in the negative region *(**Noise Signature I**)* corresponded with the Oxidation Stage
- The noise signature of quick potential continuously approaching more positive values *(**Noise Signature II**)* correlated to the External Sulfidation Stage.
- The noise signature of positive potential fluctuating randomly in a narrow range *(**Noise Signature III**)* corresponded with the Internal Sulfidation Stage

Electrochemical Current Noise Signals

- The noise pattern of the noise signature of current fluctuating with no sudden spike correlated to the Low Extent of Oxidation/Sulfidation *(**Noise Signature IV**)*.
- The noise pattern of sudden change in current values followed by slow or no recovery corresponded with the Accelerated Oxidation/Sulfidation *(**Noise Signature V**)*. These signatures can be seen clearly at 750 °C, in the flue gas without SO_2 as well as deep coal ash.

Aung, Naing Naing, and **Xingbo Liu*.** Corrosion science 82 (2014): 227-238.

Publications in Peer-Reviewed Journals

Corrosion Science 65 (2012) 1–4

Contents lists available at SciVerse ScienceDirect

Corrosion Science

journal homepage: www.elsevier.com/locate/corsci

Letter

High temperature electrochemical sensor for in situ monitoring

Naing Naing Aung, Xingbo Liu*

Mechanical and Aerospace Engineering Department, West Virginia University, Morgantown, WV 26506, USA

Article history:
Received 10 July 2012
Accepted 4 August 2012
Available online 10 August 2012

Keywords:
A. Superalloys
A. Molten salts
C. High temperature corrosion
C. Hot corrosion

Corrosion Science 76 (2013) 390–402

Contents lists available at SciVerse ScienceDirect

Corrosion Science

journal homepage: www.elsevier.com/locate/corsci

Effect of SO_2 in flue gas on coal ash high temperature electrochemical

Naing Naing Aung, Xingbo Liu*

Mechanical and Aerospace Engineering Department, West Virginia University

Article history:
Received 15 February 2013
Accepted 5 July 2013
Available online 15 July 2013

Keywords:
A. Superalloys
A. Molten salts
B. EIS
B. Polarization
B. SEM
C. Hot corrosion

Corrosion Science 82 (2014) 227–238

Contents lists available at ScienceDirect

Corrosion Science

journal homepage: www.elsevier.com

Effect of temperature on coal ash hot corrosion res of Inconel 740 superalloy

Naing Naing Aung, Xingbo Liu*

Mechanical and Aerospace Engineering Department, West Virginia University, Morgantown, WV 26506, USA

Article history:
Received 26 July 2013
Accepted 22 January 2014
Available online 30 January 2014

Keywords:
A. Superalloys
A. Molten salts
B. Polarization
B. SEM
B. Weight loss
C. Hot corrosion

1. Introduction

Ni-based superalloys are expected to be the best candidates for Advanced-Ultrasupercritial (A-USC) steam boiler applications in coal-fired power generation system. The goal of A-USC is to generate 760 °C steam although the metal surface temperature of the key components such as the superheater and reheater tubes will be 800 °C or even higher [1]. Currently, a new nickel-based superalloy, Inconel alloy 740, is under development to meet these stringent material targets. Superheater and reheater materials in the coal-fired boiler environment always suffer coal ash hot corrosion at elevated temperatures [2–18]. Thus, it is of considerable industrial interest to develop hot corrosion resistant Ni-based superalloys.

Coal ash hot corrosion is the result of competition between oxidation and sulfidation which affect alloys exposed to high temperature combustion gases containing sulfate coal ash. The shifting conditions between oxidation and sulfidation can greatly vary the corrosion rate as a consequence of slow-growing oxide scale and fast-growing sulfide scale [13]. Operating temperature is one of the important factors that influence sulfidation tendency in coal ash hot corrosion of Ni-based superalloys. A high sulfidation tendency can be observed in the low temperature form of hot corrosion (Type II hot corrosion) due to the formation of low-melting alkali sulfate eutectic mixtures [6,7,10–13]. This is the reason

* Corresponding author. Tel.: +1 304 293 3339; fax: +1 304 293 6689.
E-mail address: xingbo.liu@mail.wvu.edu (X. Liu).

ISA Transactions 55 (2015) 188–194

Contents lists available at ScienceDirect

ISA Transactions

journal homepage: www.elsevier.com/locate/isatrans

Development of self-powered wireless high temperature electrochemical sensor for in situ corrosion monitoring of coal-fired power plant

Naing Naing Aung[a], Edward Crowe[b], Xingbo Liu[a,*]

[a] Mechanical and Aerospace Engineering Department, West Virginia University, Morgantown, WV 26506, USA
[b] National Research Center for Coal and Energy, West Virginia University, Morgantown, WV 26506, USA

Article history:
Received 7 May 2014
Received in revised form
31 July 2014
Accepted 9 September 2014
Available online 3 October 2014
This paper was recommended for publication by He Peter

Keywords:
High temperature electrochemical sensor
In situ corrosion monitoring
Wireless communication
Thermoelectric generator

ABSTRACT

Reliable wireless high temperature electrochemical sensor technology is needed to provide in situ corrosion information for optimal predictive maintenance to ensure a high level of operational effectiveness under the harsh conditions present in coal-fired power generation systems. This research highlights the effectiveness of our novel high temperature electrochemical sensor for in situ coal ash hot corrosion monitoring in combination with the application of wireless communication and an energy harvesting thermoelectric generator (TEG). This self-powered sensor demonstrates the successful wireless transmission of both corrosion potential and corrosion current signals to a simulated control room environment.

1. Introduction

Increasing global energy demands, coupled with an ageing and inefficient fleet of power generation plants will require the deployment of next-generation ultra-supercritical (USC) coal-fired power plants [1,2]. One of the major hurdles in the development of USC power generation systems is managing coal ash hot corrosion which can lead to sudden catastrophic failure of USC boiler tubes [3–5]. An effective approach to improve reliability is to apply robust, in situ high temperature corrosion monitoring sensors to provide real time corrosion information so that the catastrophic failure can be prevented. Energy harvesting wireless sensor systems are more easily implemented with lower installation costs than traditional grid-powered sensors applied in harsh corrosion environments [6–8].

Combining the concept of energy harvesting and state-of-the-art wireless communication technology creates a nearly service-free data transmission system. In this case, a thermoelectric generator (TEG) is used as an energy harvester utilizing the heat transferred between the heat source and ambient air to generate electricity. TEGs are rugged, reliable, solid-state devices that convert heat directly into electricity [9–11]. They produce a constant power output for a given temperature difference between their hot and cold sides, can operate at elevated temperatures with supplementary cooling, and have proven to be reliable in various applications including harsh environments. A coal-fired boiler environment can provide the thermal energy necessary to produce sufficient power for robust, commercially available wireless instrumentation.

There are three major types of corrosion measurements that can be considered for use in high temperature corrosive environments: (1) the first type is a corrosion sensor where an alloy coupon would be incorporated into the *weight loss* test for a fixed period of time. It provides a quantitative corrosion rate, but the value only represents average corrosion over the fixed time period; (2) the second type is based on the *electrical resistance* of the sensor which measures the decrease in thickness of the sensor material as an increase in the sensor resistance. The data are very dependent on accurate temperature measurements and cannot distinguish localized corrosion; (3) a third type is one based on the measurement of *electrochemical signals*. These signals should be directly proportional to the corrosion rate and come in the form of linear polarization resistance (LPR), electrochemical impedance spectroscopy (EIS), and electrochemical noise analysis (ENA). Recently, it has been demonstrated that our novel high temperature electrochemical sensor can detect the hot corrosion

* Corresponding author. Tel.: +1 304 293 3339.
E-mail address: xingbo.liu@mail.wvu.edu (X. Liu).

Sensor Testing @ Prototype Boiler

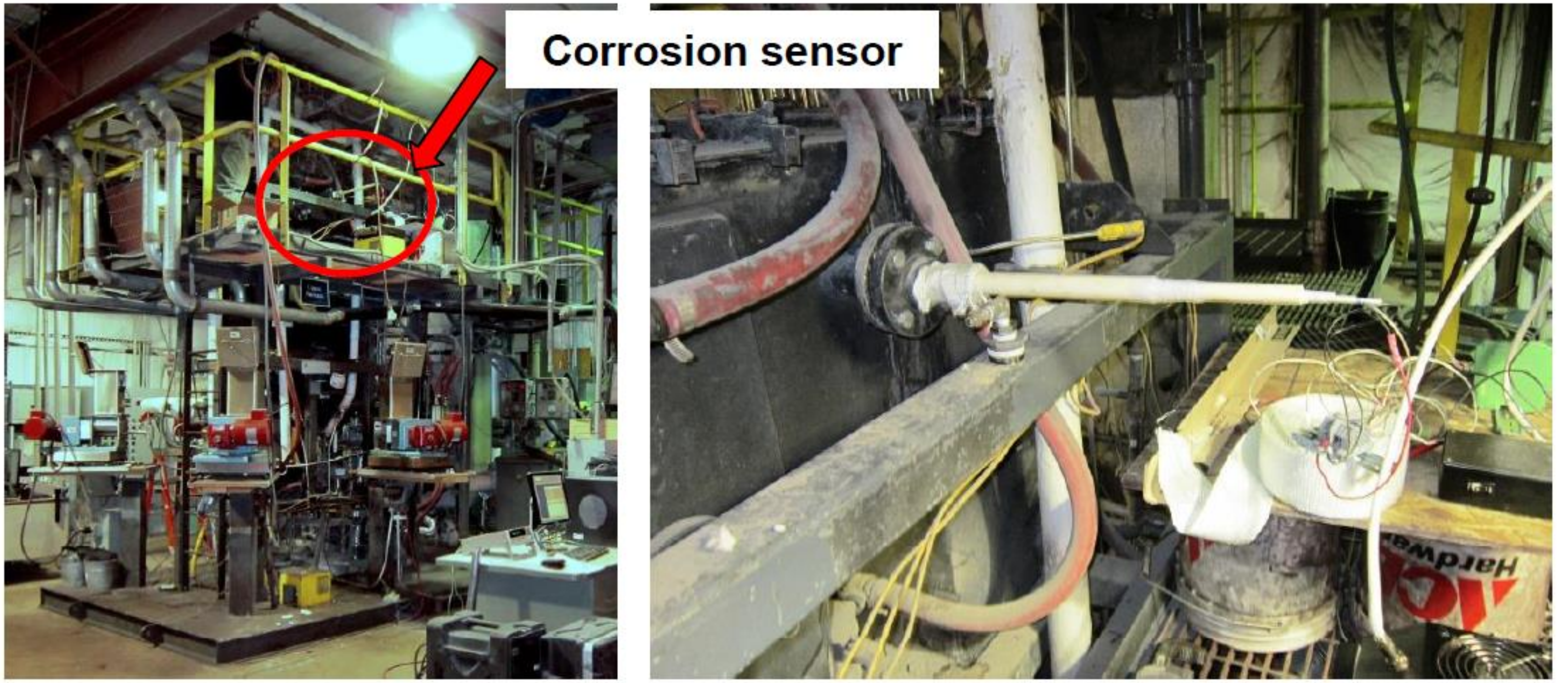

Fig. 3 Corrosion and Wireless Sensor Location at WRI's Combustion Test Facility

Photographs of WVU high temperature corrosion sensor: (a) new sensor; (b) sensor 45 days post-exposure in boiler at WRI's Combustion Testing Facility

Project Objectives

- To validate the effectiveness of our Recipient's lab-scale electrochemical sensor for high temperature (HT) corrosion in coal-based power generation boilers;
- To optimize the Recipient's HT sensor (currently at technology readiness level TRL-5) to reach TRL-6;
- To develop a pathway toward commercialization of such technology.

Planned Tasks & Deliverables

ID	Task	Year 1				Year 2				Year 3			
		Q1	Q2	Q3	Q4	Q1	Q2	Q3	Q4	Q1	Q2	Q3	Q4
1	Project management	■◆	■	■	■	■	■	■	■	■	■	■	■
2	Sensor development & optimization												
2.1	Design & construct sensors	■	■			■	■			■	■		
2.2	Sensor packaging		■	■			■	■			■	■	
3	Signal processing & communication instruments		■	■			■	■			■	■	
4	Corrosion sensor testing @ Longview Power's boiler												
4.1	Sensor placement and installation			■				■				■	
4.2	Sensor testing			■	■◆			■	■			■	■
4.3	Post-mortem analyses				■	■			■	■			■
5	Corrosion monitoring software & database development												
5.1	Lab-scale sensor optimization	■	■			■	■			■	■		
5.2	Electrochemical and corrosion monitoring validation		■	■			■	■			■	■	
5.3	Post-mortem analysis			■	■			■	■				■
5.4	Database and predictive model development			■	■			■	■			■	■
5.5	Software development			■	■			■	■◆			■	■
6	Tech-transfer & commercialization												
6.1	NPV model & uncertainty analysis	■	■	■	■	■	■◆	■	■			■	■
6.2	NEMS model and economic analysis							■	■	■	■	■◆	■
6.3	Commercialization pathway development						■	■			■	■	■

- Y1-Q1, finish updating PMP
- Y1-Q4, demonstrate the high temperature corrosion sensor can withstand the harsh environment in Longview's A-USC boiler.
- Y2-Q2, complete the NPV model and uncertainty analysis
- Y2-Q4, complete the electrochemical and corrosion database and model construction
- Y3-Q2, complete the NEMS model and economic analysis

Sensor Testing @ Longview Power Plant

Location	Monongalia County near Maidsville, WV
Status	Operational
Commission date	2011
Owner(s)	Longview Power
Thermal power station	
Primary fuel	Coal and natural gas
Type	Steam turbine
Power generation	
Nameplate capacity	700 MW

- Officially a "zero discharge" power plant in WV
- Includes a new air pollution control system that results in emissions that is among the lowest in the nation for coal plants.
- Emits less CO_2 than most other coal-fired power plants because of its high fuel efficiency.

Sensor Testing Locations

Superheater/reheater tubes working conditions: high temperature and pressure (550-750^{o}C, 30MPa), high salt concentration (Na_2SO_4,K_2SO_4), corrosive flu gas (O_2, SO_2 and SO_3)

Component: Nickel-based alloys (e.g., 282, 740) or fire-resistant stainless steel (e.g., 347H).

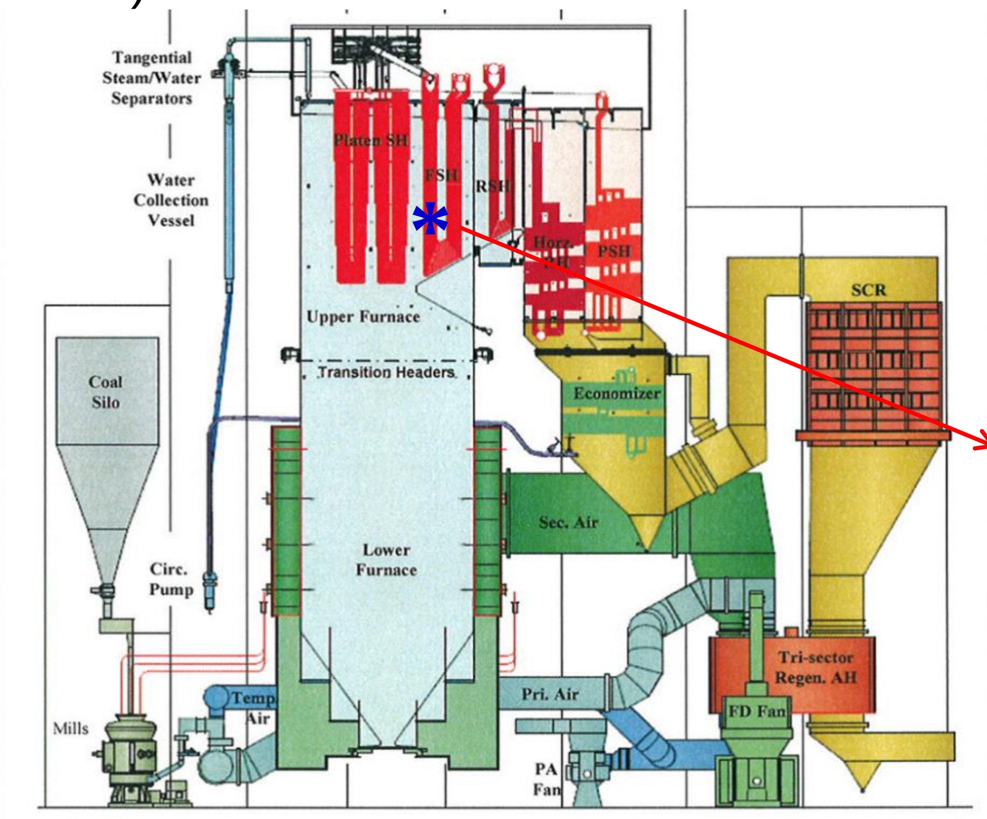

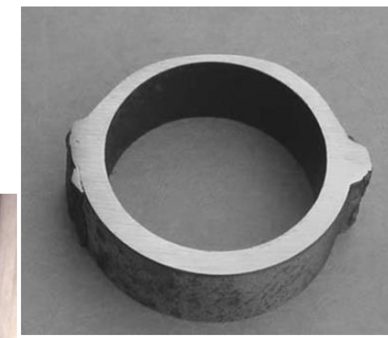

Fire side

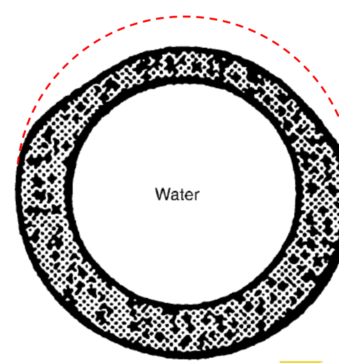

ECN Corrosion Sensor Design

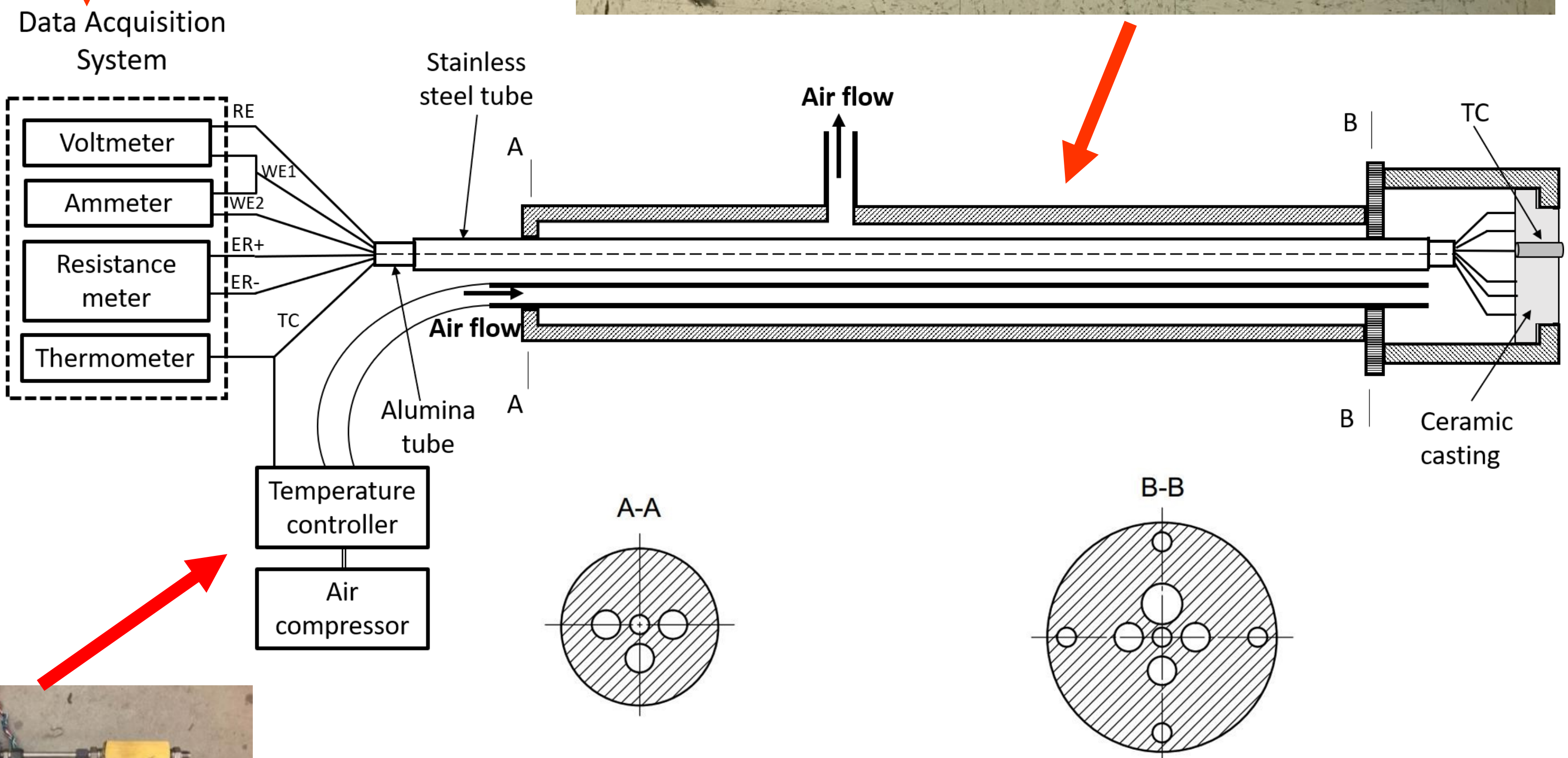

Sensor Packaging-Data Acquisition System

- ✓ This data acquisition system has a reliable accuracy.
- ✓ The latest version also enables remote data collection (developed in Feb 2020).

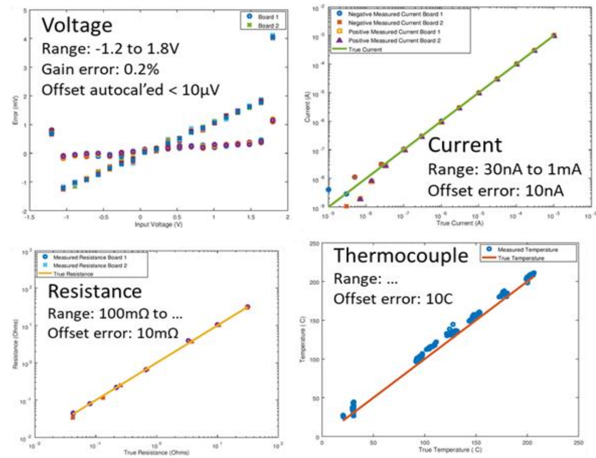

[Left] PIECES hardware. (a) Top view of the fully-assembled device. (b) Bottom view of the Front Panel. (c) Top view of the Measurement Board. [Right] Verification of each measurement type.

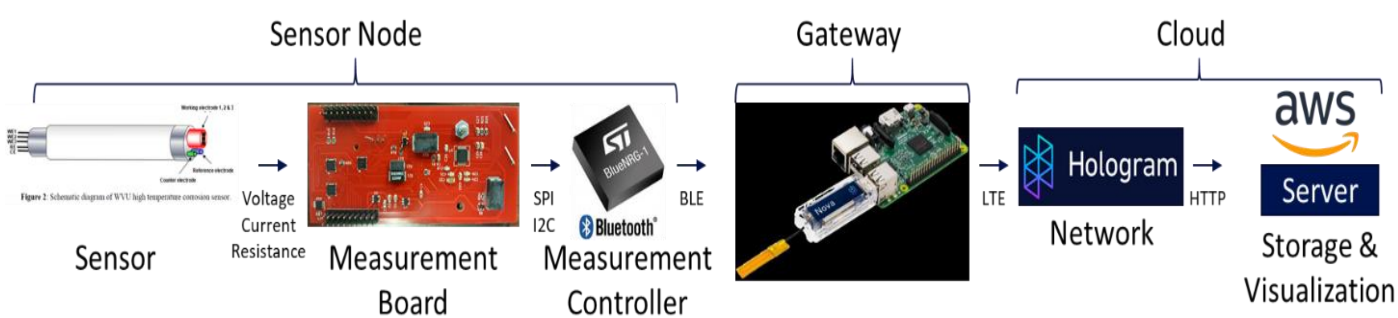

Envisioned data pipeline for the corrosion sensor.

Sensor Packaging-Data Acquisition

- ✓ Easy access to real-time data stored in the Cloud

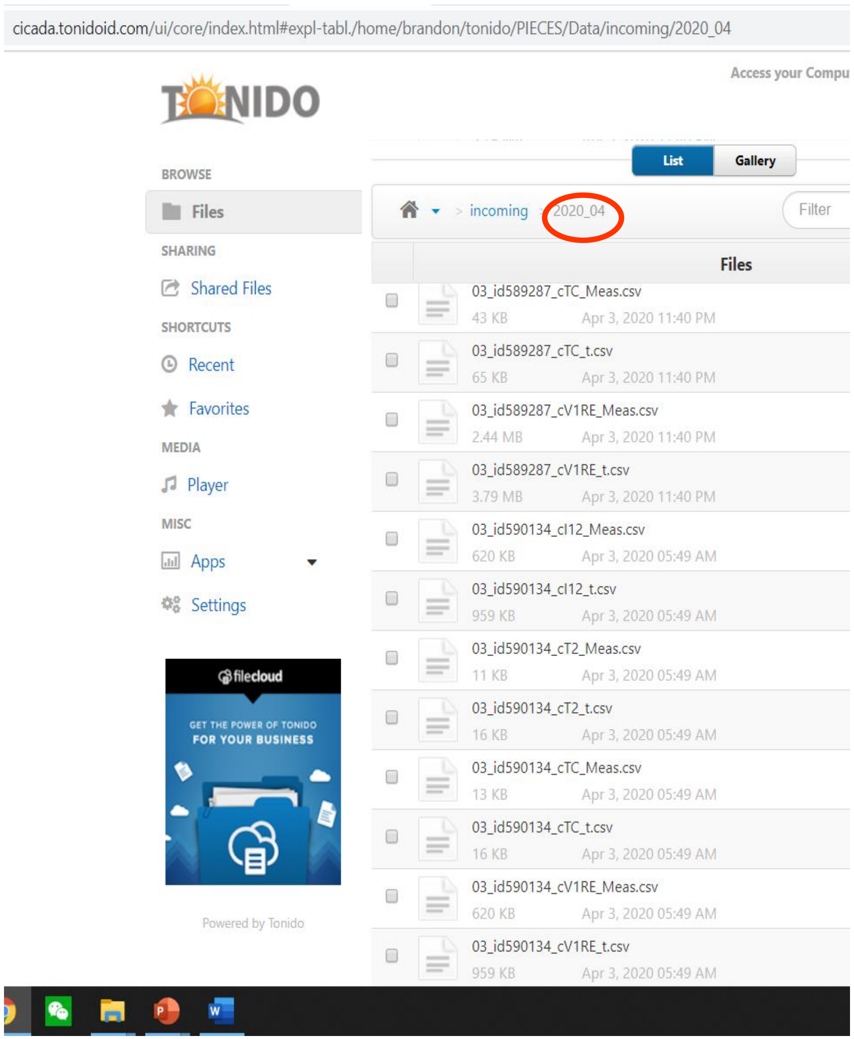

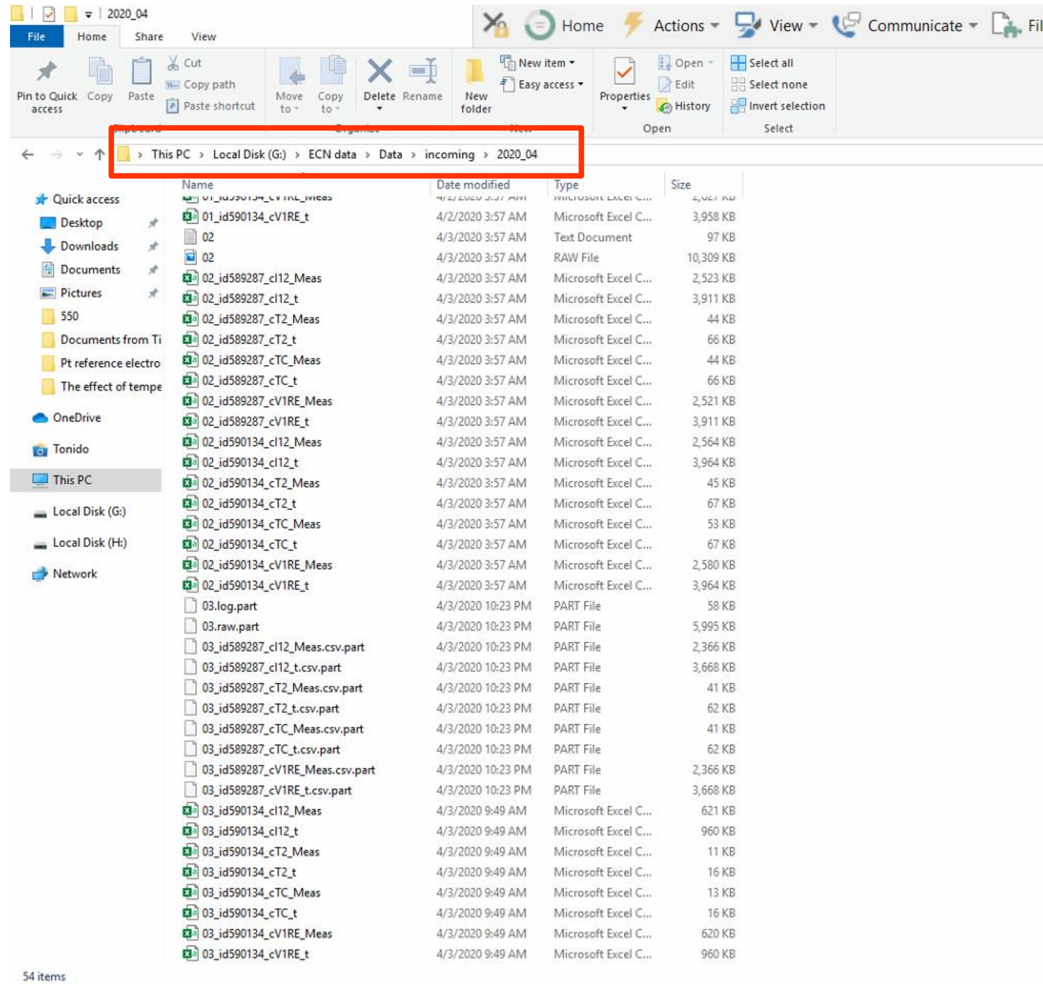

Sensor Placing and Installation-ECN Sensor

✓ An updated electrochemical sensor was successfully installed on Aug 30th, 2019

Electrochemical sensor

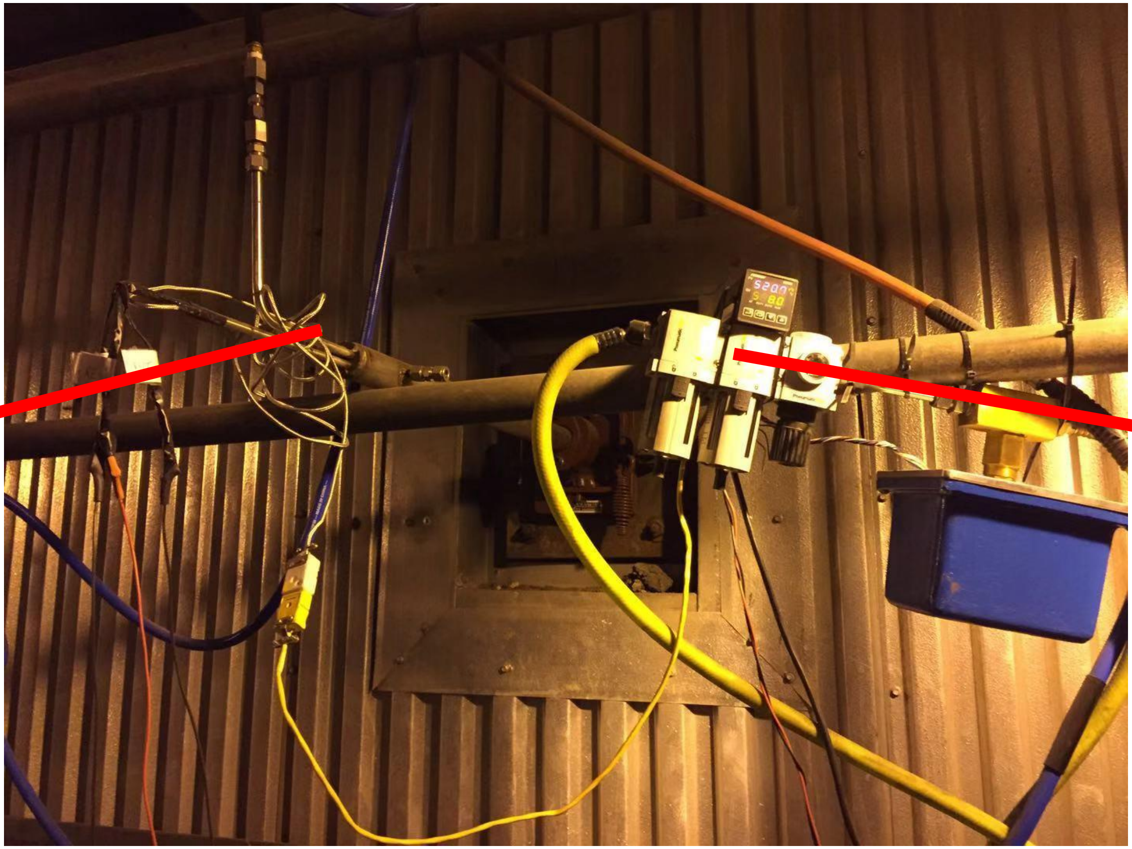

Temperature Controller (550 ^{o}C)

ECN sensor system installed through the observation port near superheater (11th floor of the boiler).

Field Measurement Results-PDP curves

- ✓ PDP curve was successfully obtained after 1d, demonstrating the formation of molten salt layer on 347H SS.
- ✓ Stern-Geary coefficient was calculated from PDP curve as 69.78.

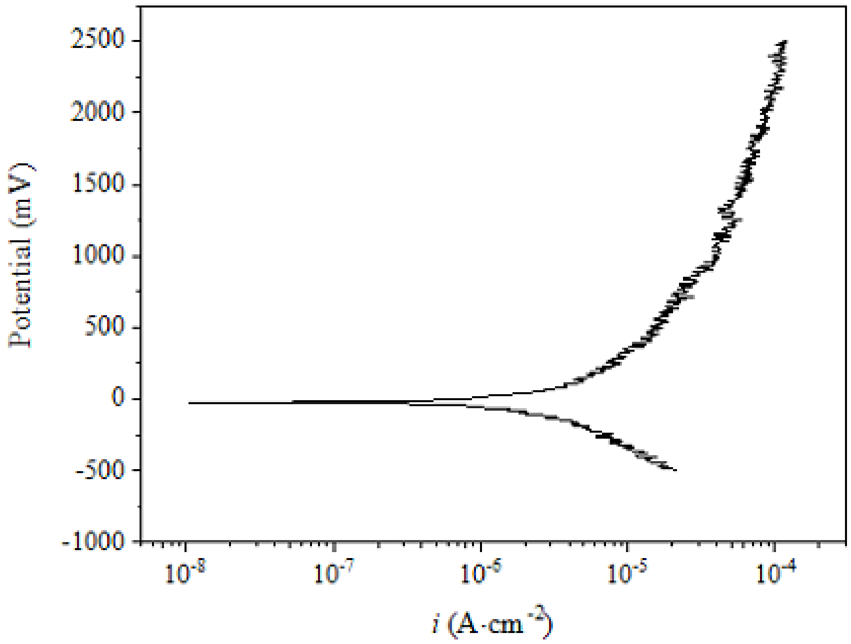

The potentiodynamic polarization (PDP) curve of 347H SS measured at superheater place (550ºC)

Parameters obtained from the PDP

Materials and location	Anodic Tafel slope, α (mV/decade)	Cathodic Tafel slope, β (mV/decade)	Stern-Geary coefficient, B (mV)
347 SS, Superheater	810.08±159.98	200.49±17.72	69.78

Anodic reaction: $Fe - 3e^{-} \rightarrow Fe^{3+}$

n=3, ρ=7.8 g/cm^3, M=56 g/mol

Predictive Model Development-Calculations of Corrosion Rate

- ✓ Corrosion depth can be calculated by EN data through eq. (6).

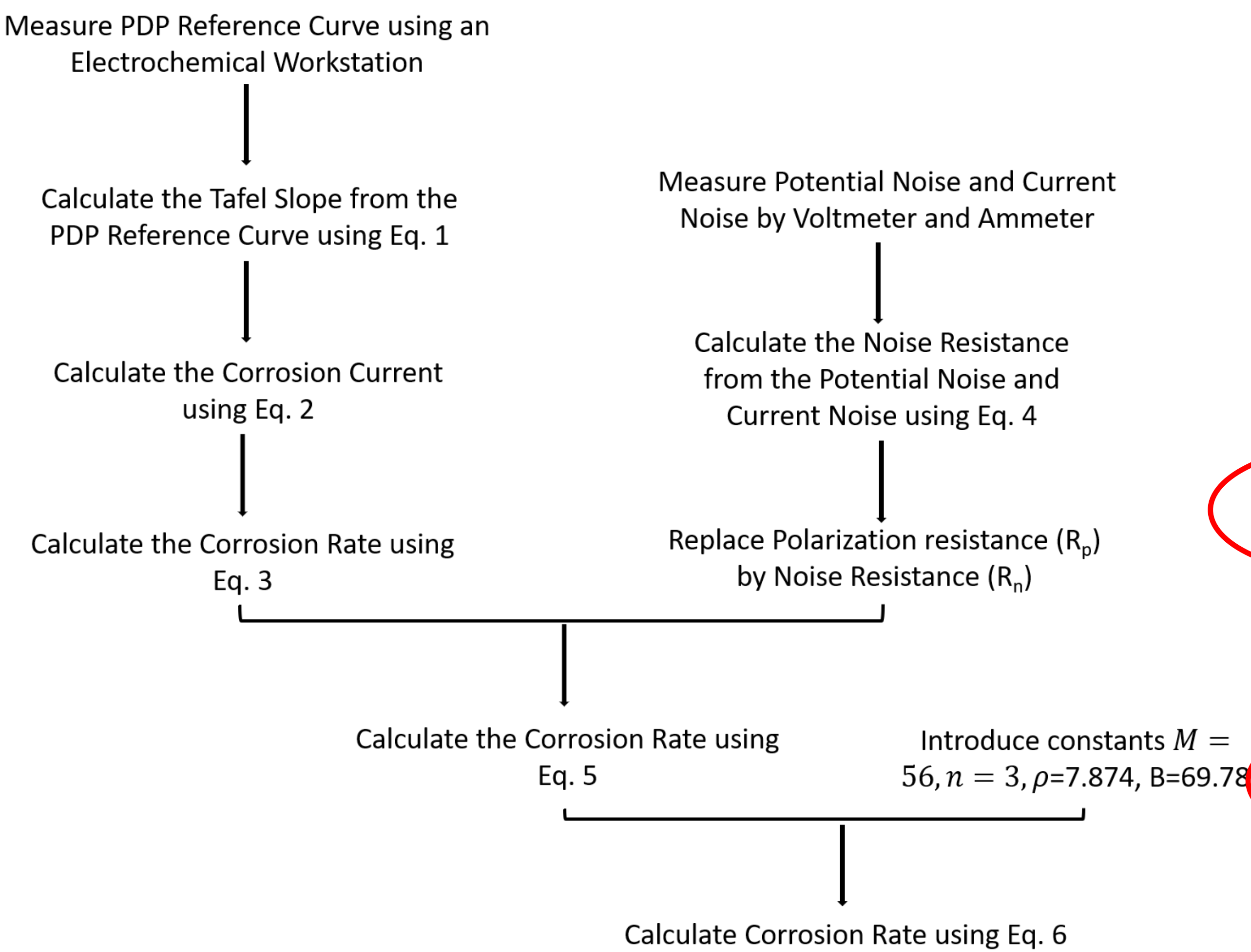

$$B = \frac{\alpha\beta}{\alpha+\beta} \quad (1)$$

$$J_{corr} = \frac{B}{R_p} \quad (2)$$

$$V_{corr} = \frac{3.27 \times B \times M}{n \times \rho \times R_p} \quad (3)$$

$$R_n = \frac{\sigma_v}{\sigma_i} \quad (4)$$

$$V_{corr} = \frac{3.27 \times B \times M}{n \times \rho \times R_n} \quad (5)$$

$$V_{corr} = \frac{540.9}{R_n} \quad (6)$$

Processes to calculate the corrosion depth by electrochemical noise data

Field Measurement Results-ECN Data

- ✓ The latest electrochemical sensor works well in the last seven month.
- ✓ EN data was successfully collected unless the boiler is down

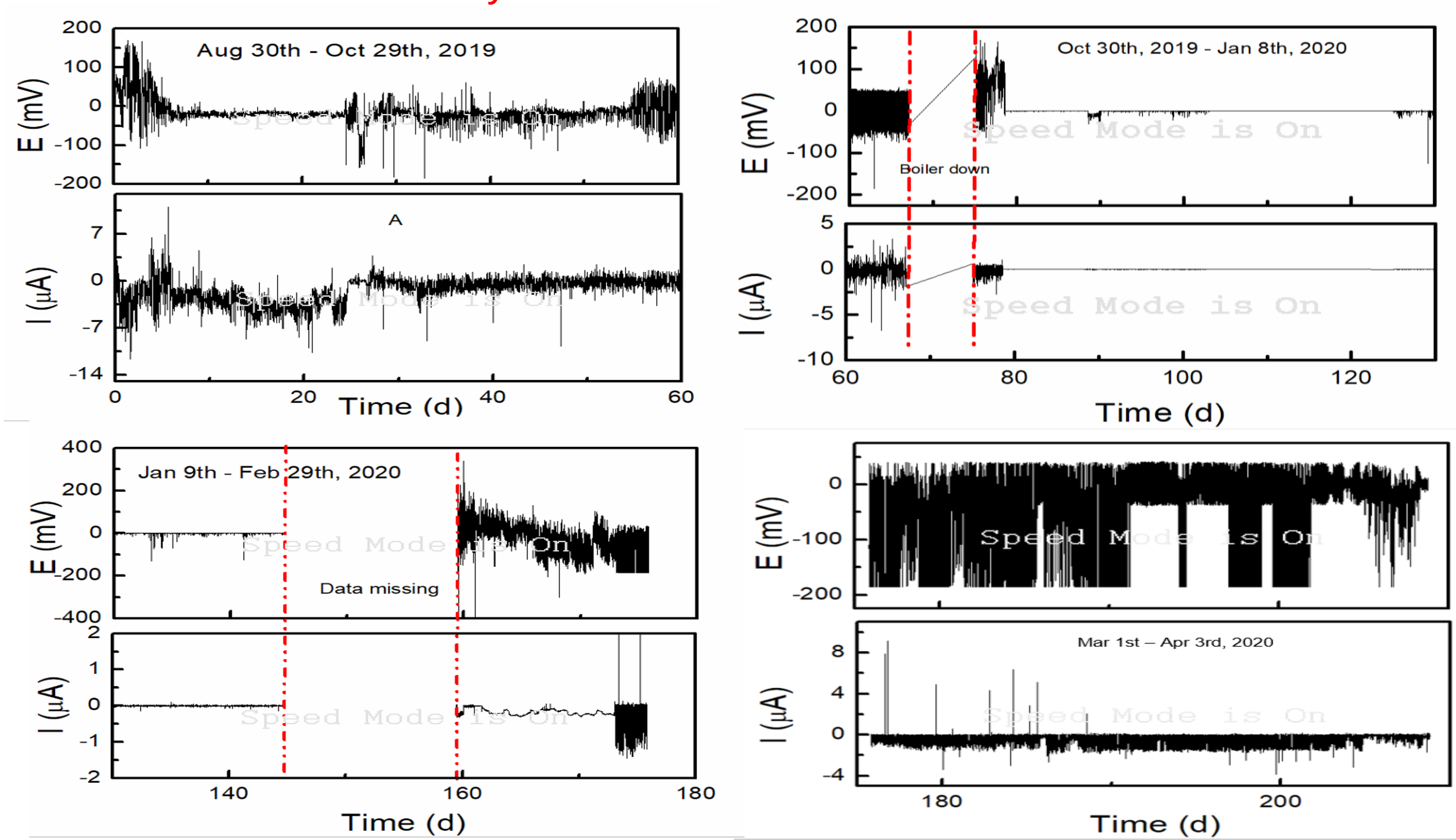

Electrochemical noises measured at the superheater (548°C) since Aug 30th, 2019.

Field Measurement Results-Data Processing

- ✓ EN data were readily converted into corrosion rate by using MATLAB.

```
clear all;% clear all existing variables
A= xlsread('29_id590134_cV1RE_Meas.csv');% read data of potentiao noise
B= xlsread('29_id590134_cI12_Meas.csv'); % read data of current noise
C= xlsread('29_id590134_cI12_t.csv');
e= 810.08; % anodic tafel slope
f= 200.49; % cathodic tafel slope
g= e*f/(2.303*(e+f)); %stern-Geary coefficient
i=1;j=1;
D=ones();
while (i< length(C)-2047)
    X=C(i+1023)-C(1);%choose time segment with size of 2048
    Yp=A(i:i+2047);%choose potential segment with size of 2048
    yp=detrend(Yp);%Remove trend of potential noise
    a=std(yp);%calculate standard deviation of trend-removed potential noise
    Yc=B(i:i+2047);%choose potential segment with size of 2048
    yc=detrend(Yc);%Remove trend of current noise
    b=std(yc);%calculate standard deviation of trend-removed current noise
    d=std(Yc);%calculate standard deviation of current noise
    c=sqrt(sum(yc).^2/length(yc));%alcualte the root mean square of current noise
    Rn=a/b;%calculate noise resistance
    PI=b/c;%calculate localized index
    Vcorr=7.75*g/(0.95*Rn);%calculate corrosion rate
    D(j,1)=X/3600/24;%output time value with unit of day
    D(j,2)=Rn;%output noise resistance value
    D(j,3)=PI;%output localized corrosion index
    D(j,4)=Vcorr;%output corrosion rate
    j=j+1;
    i=i+2048;
end
CD=cumtrapz(D(:,1)/365,D(:,4));%calculate accumlated corrosion depth
D(:,5)=CD;
subplot(2,2,1)
plot(D(:,1),D(:,2))
xlabel('time (d)')
ylabel('Rn (Ohm;¤cm^2)')
title ('Noise resistance')
subplot (2,2,2)
plot(D(:,1),D(:,3))
xlabel('time (d)')
ylabel('Localized index')
subplot(2,2,3)
plot(D(:,1),D(:,4))
xlabel('time (d)')
```

Time	Corrosion depth
0.0061	0
0.0182	8.6030e-08
0.0304	1.6822e-07
0.0425	2.0654e-07
0.0547	2.3728e-07
0.0669	2.6871e-07
0.0790	3.1839e-07
0.0913	3.7530e-07
0.1035	4.2233e-07
0.1156	4.6193e-07
0.1277	4.9972e-07
0.1398	5.3956e-07
0.1520	5.7234e-07
0.1641	6.0372e-07
0.1762	6.4083e-07
0.1883	6.7826e-07
0.2005	7.1990e-07
0.2126	7.6299e-07
0.2248	7.9969e-07
0.2369	8.3652e-07
0.2490	8.7532e-07
0.2612	9.1110e-07
0.2733	9.5186e-07
0.2854	9.9646e-07
0.2975	1.0338e-06
0.3097	1.0768e-06
0.3218	1.1371e-06
0.3339	1.1893e-06
0.3461	1.2270e-06
0.3583	1.2676e-06
0.3704	1.3132e-06
0.3826	1.3618e-06
0.3959	1.5686e-06
0.4081	1.7507e-06
0.4202	1.7889e-06

Field Measurement Results – Corrosion Rates

✓ The corrosion depth calculated by EN data is about mm in last six month.

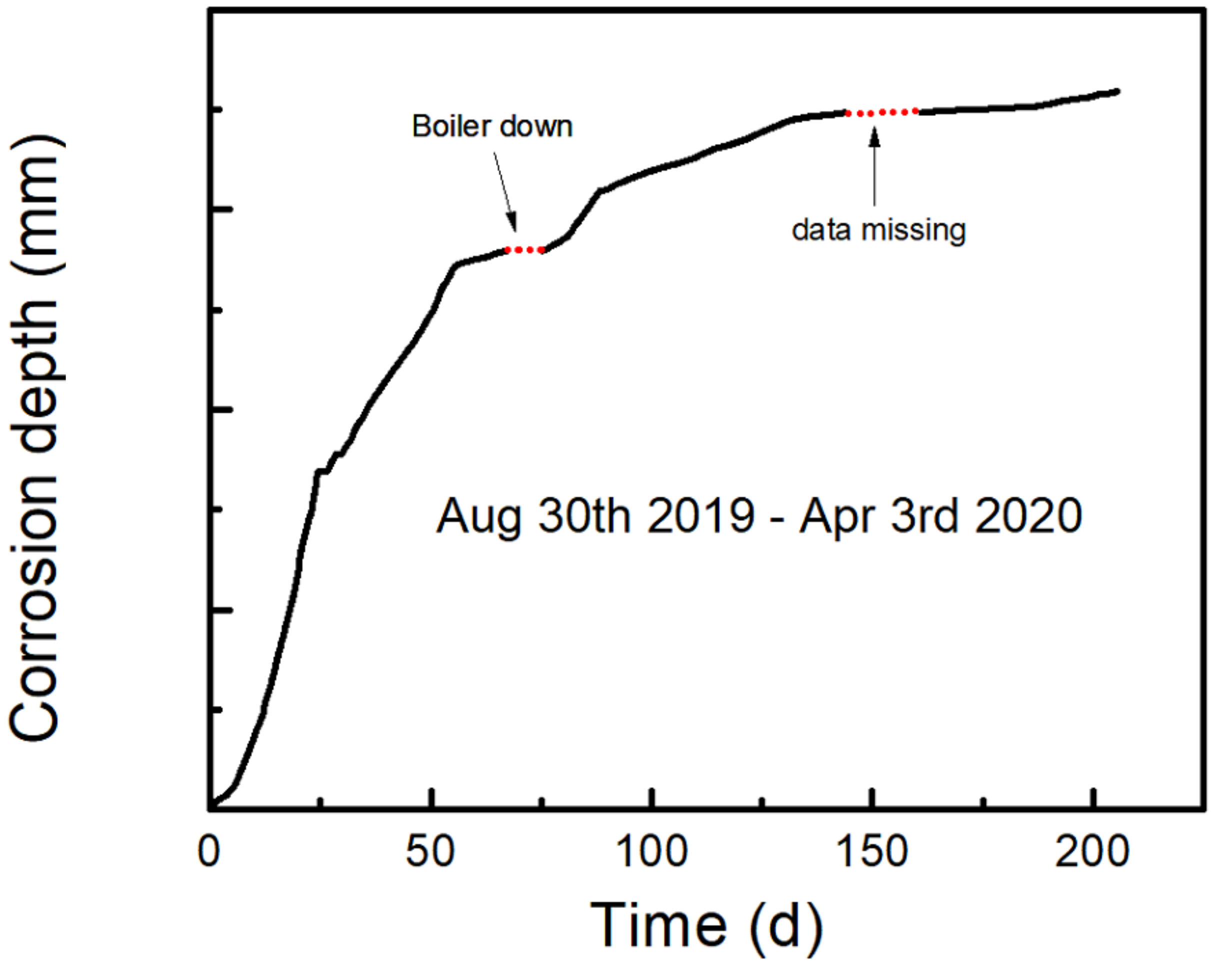

Time dependence of the accumulated corrosion depth calculated from the electrochemical noises measured at the superheater place.

Corrosion Database Development-Experiment Conditions

- ✓ Two kinds of coal ashes have different crystal structures.
- ✓ The main elements in both sets of coal ash are O, Al, Si, Fe, Ca, Na, K

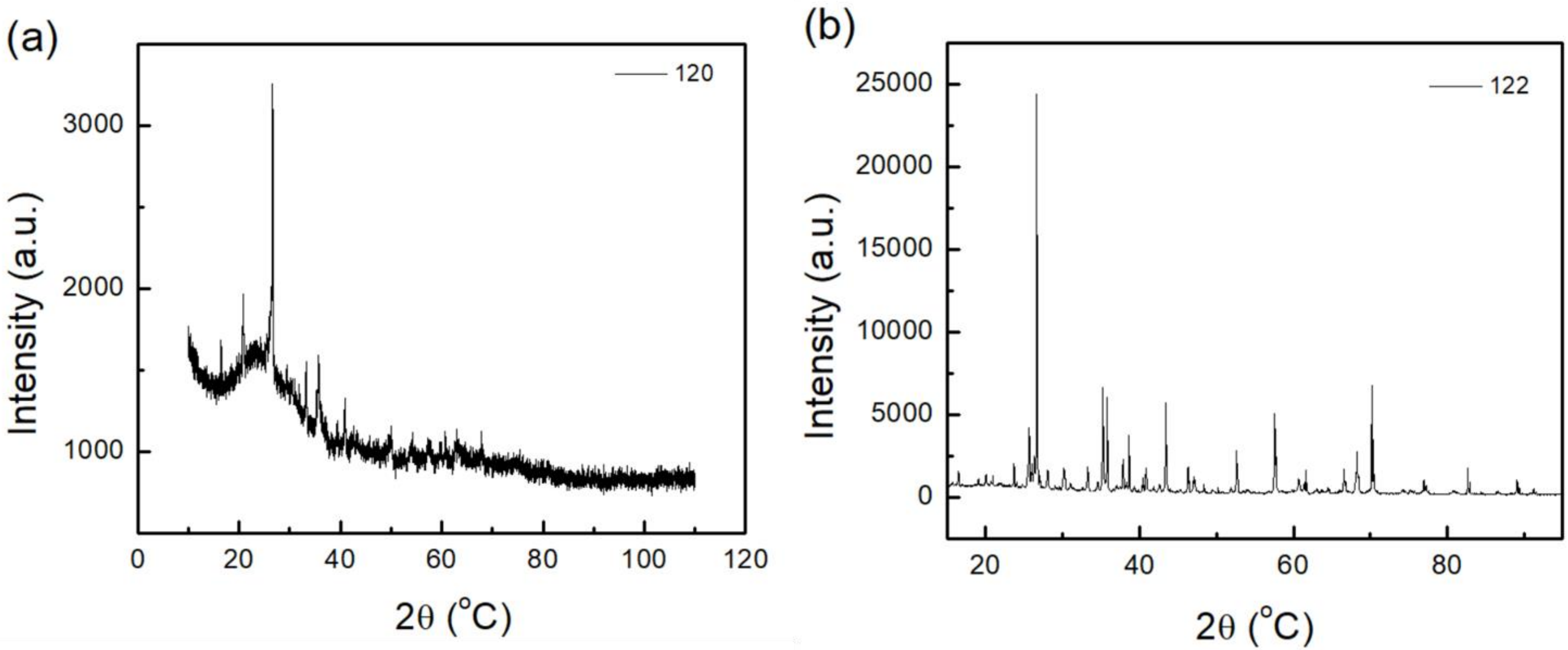

XRD pattern of two kinds of coal ashes obtained from Longview Power Plant

Corrosion Database Development-Experiment Conditions

- ✓ Some alkaline sulfate (Na_2O, K_2O and SO_3) was confirmed in both kinds of coal ashes
- ✓ Some metal oxides are found in both coal ashes
- ✓ Analysis result is similar to others reported in the literature

Various oxides in two kinds of coal ashes from Longview

	Al_2O_3	CaO	Fe_2O_3	MgO	MnO	P_2O_5	K_2O	SiO_2	Na_2O	SO_3	TiO_2
120	20.88	5.18	11.82	1.15	0.05	0.23	2.26	49.17	0.64	0.92	0.99
122	61.46	2.33	0.62	0.08	0.01	0.20	0.10	27.81	0.21	0.08	1.38

Representative chemical compositions of the coal ash in Literature

Al_2O_3	Fe_2O_3	SiO_2	Na_2SO_4	K_2SO_4	NaCl	$CaSO_4$
30	30	30	5	5		
29.25	29.25	29.25	5.625	5.625	1	
22	6	39	2	2		29

Corrosion Database Development- Experiment Conditions

- ✓ Experiment conditions (gas composition and coal ash composition) were decided based on the analysis result and reported data in literature.
- ✓ 347H, component of the superheater, was obtained from Longview Power Plant

Representative chemical composition of the flue gas in literature

N_2	CO_2	SO_2	O_2	H_2O	HCl
81.25	15	0.25	3.5		
80	15	1	4		
Bal.	13.4	1300 vpm	4	8.6	400 vpm
80	10	1.5	3.5	5	
82.9	14	0.1	3		

Element composition of the 347H obtained from Longview Power Plant

Element	C	Mn	P	S	Si	Cr	Ni	Mo	Nb	Fe
Weight ratio (%)	0.041	1.75	0.02	0.003	0.32	17.52	9.22	0.26	0.71	Bal

Corrosion Database Development-Effect of Temperature

- ✓ OCP increases by time because of the growth of passive film
- ✓ This reference electrode can provide a stable potential at this working environment.

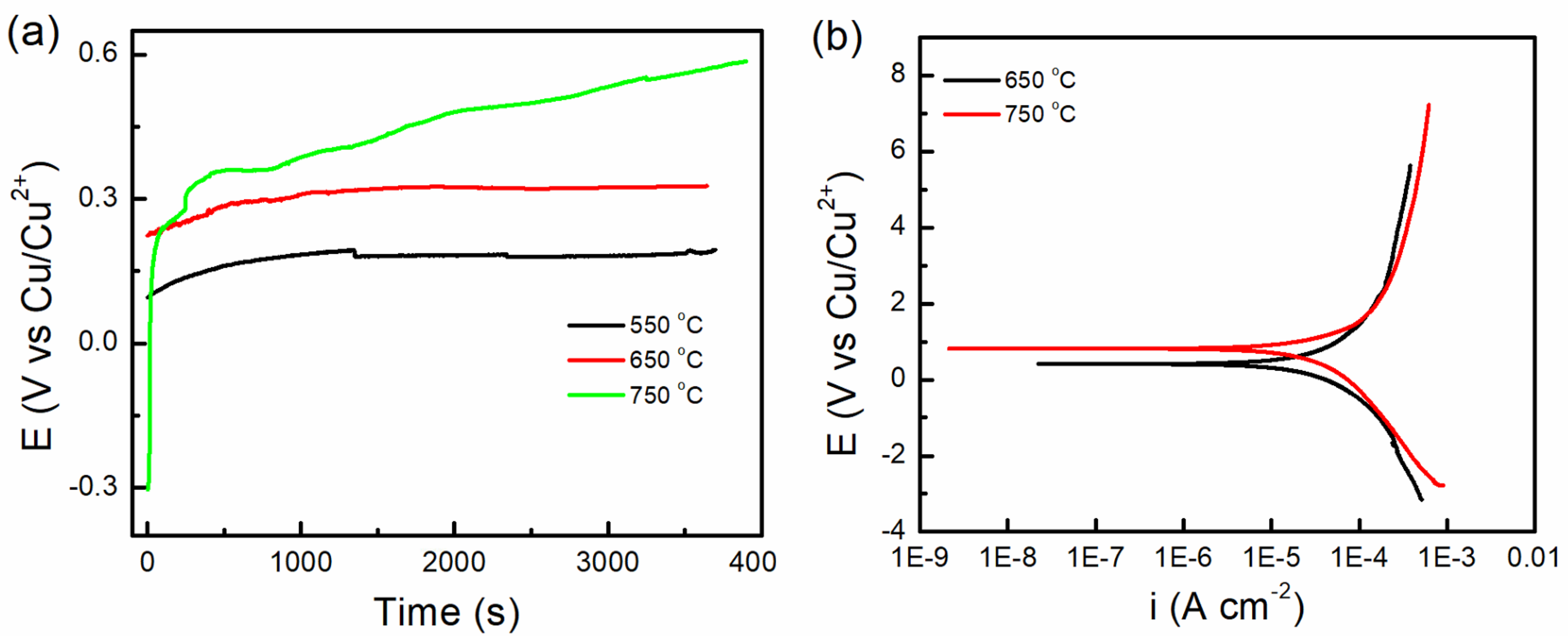

(a) OCP of 347H in the first 1h and (b) potentiodynamic polarization curve (PDP) at various temperature

Corrosion Database Development -Effect of Temperature

- ✓ Potential noise reveals two stages of the corrosion process: oxidation from 1 to 49h, sulfidation after 49h.
- ✓ Current noise needs to be verified again.

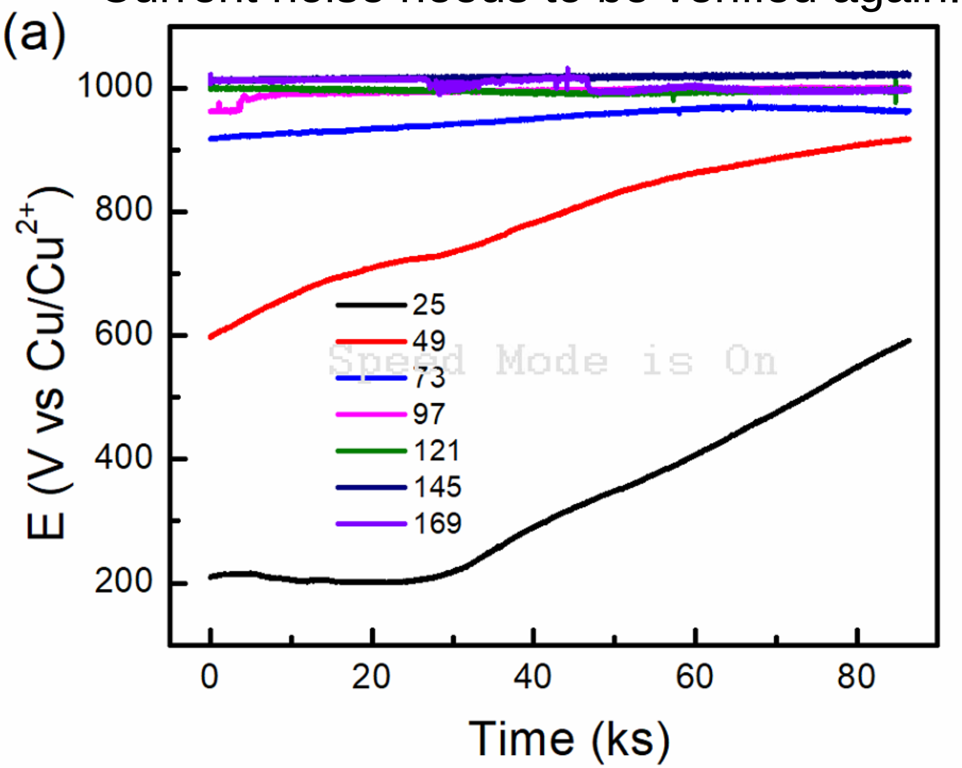

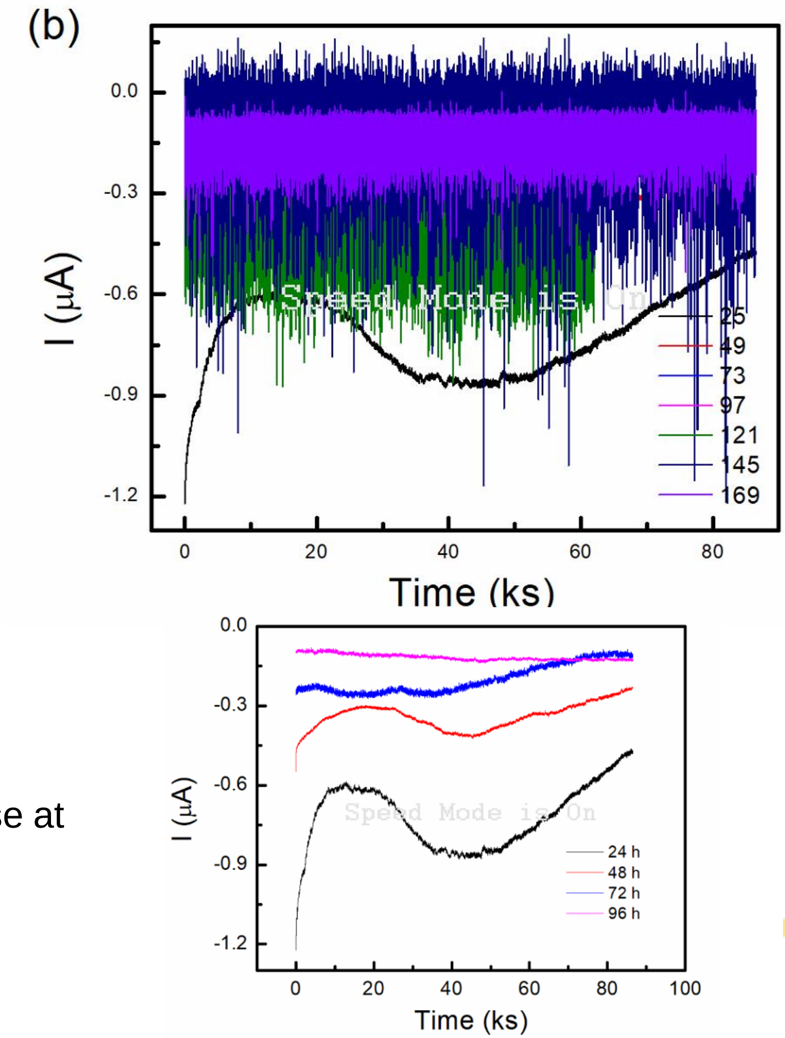

Time sequences of (a) potential and (b) current noise at 550 ^{o}C in a 7d exposure period

Corrosion Database Development-Effect of Temperature

- ✓ Corrosion resistance varies by time at 550 ºC.
- ✓ R_n and R_{sn} show the same trend.

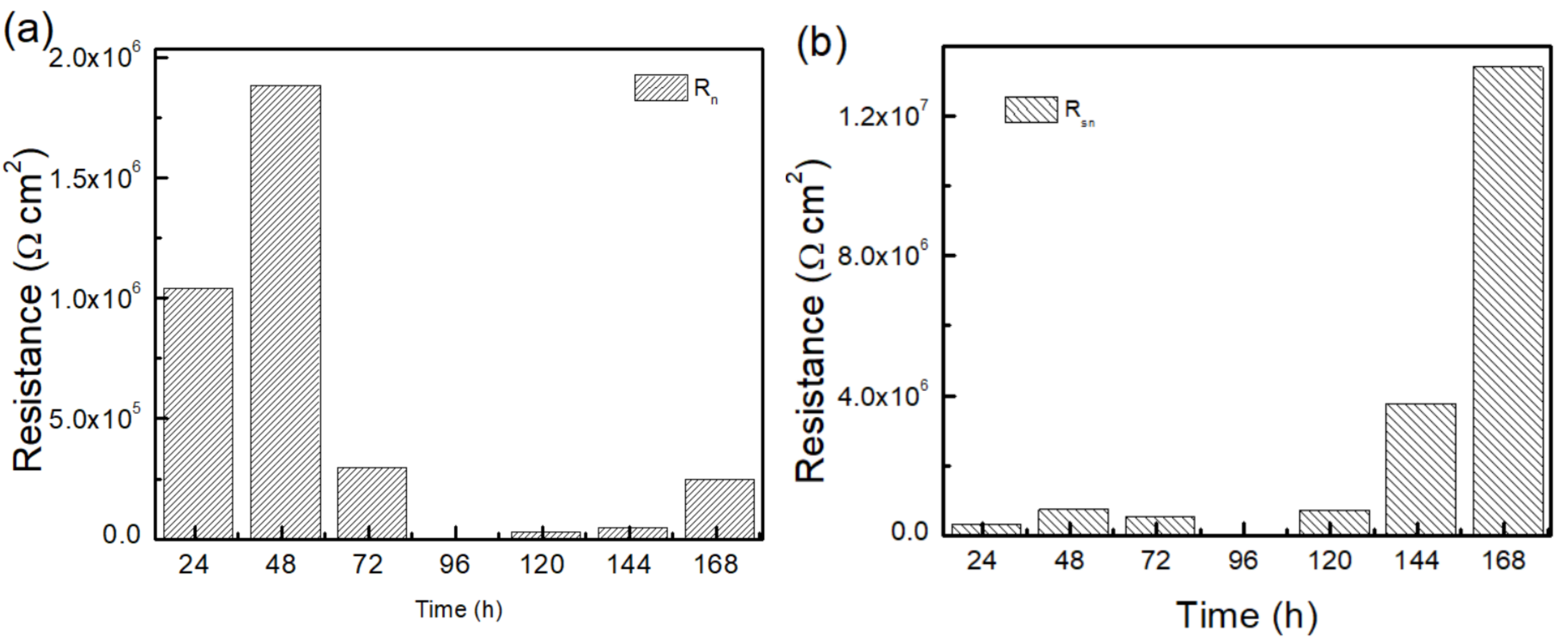

Variation of (a)R_n and (b)R_{sn} at different exposure time at 550 ºC

Corrosion Database Development-Effect of Temperature

- ✓ Localized corrosion occurs at 550 ºC

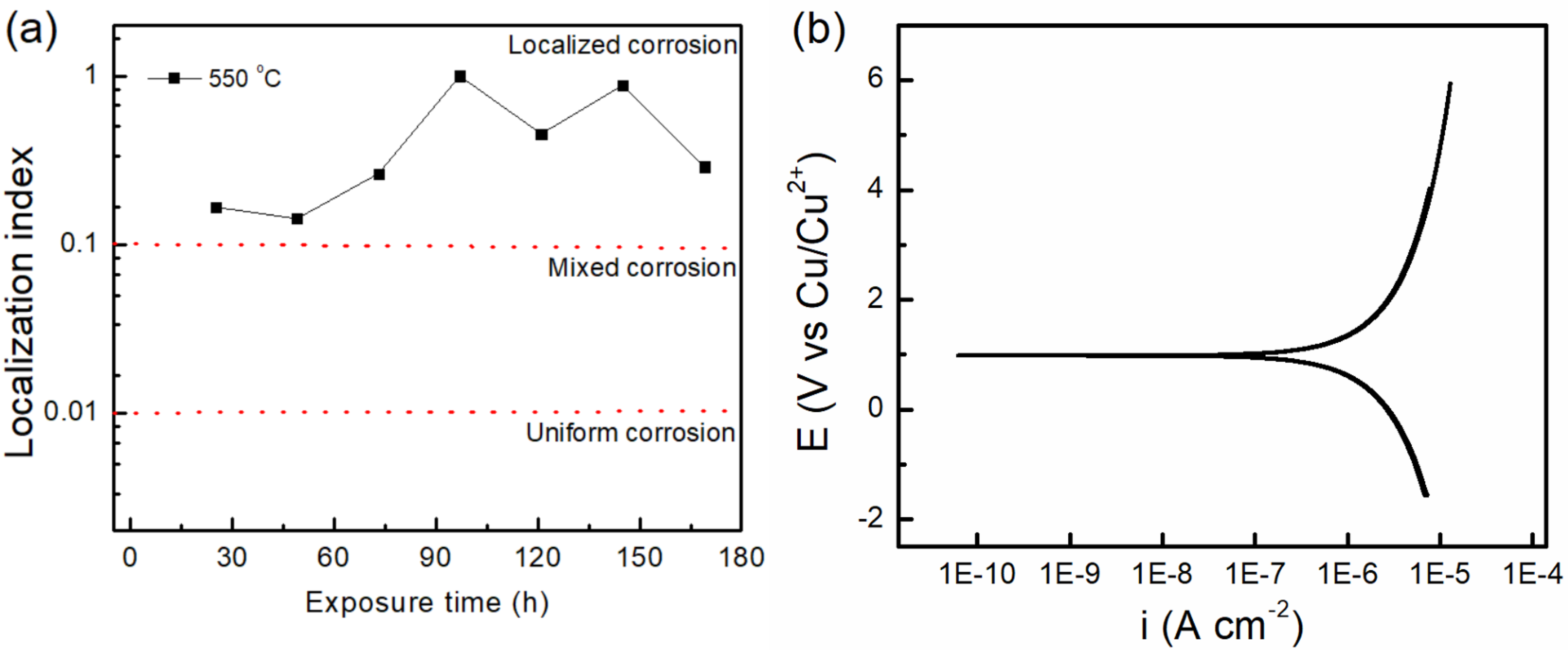

(a) Localization index at various exposure time and (b) PDP curve after 7d exposure at 550 ºC

Techno-Economic Analysis - Motivation

- ✓ As per State of Reliability (SOR) report by North American Electric Reliability Council (NERC), waterwall failure accounts for about 6-7% of the production lost due to forced outages over past several years.

- ✓ Revenue lost due to forced outages in larger power plants is significantly higher than the smaller ones. For example, the loss in revenue in 2015 in a 1000 MW power plants was about 5 times than that of a 300 MW plant (NERC GADS, 2016). Thus large power plants such as Longview is an ideal candidate.

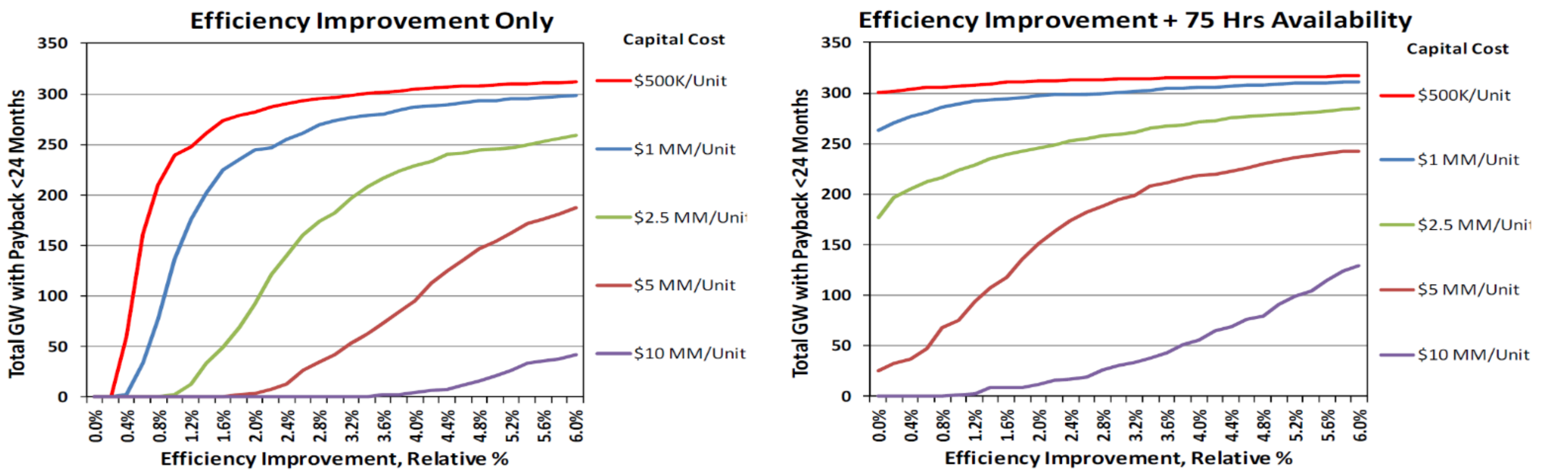

Impacts of efficiency, availability and capital cost (Krulla et al. NETL Report, DOE/NETL-342/03082013, 2013)

TEA - Approach

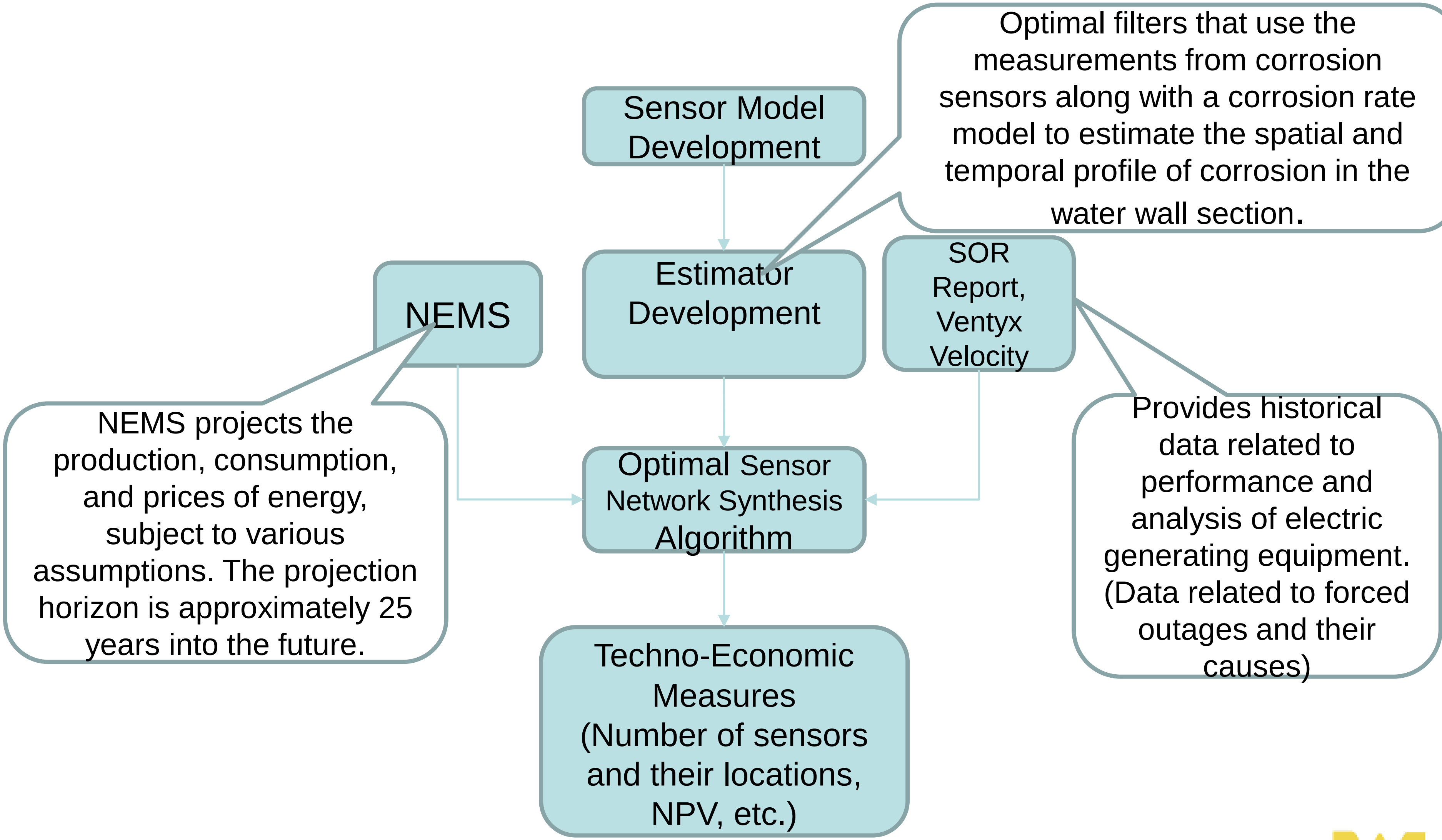

TIMES Model

- TIMES model generator is used to explore possible energy futures based on scenarios.
- A scenario is created by increasing availability of the coal fired power plants due to the use of the corrosion sensors by about 5% compared to current value.
- The electricity produced by coal fired power plants in the U.S. is computed by the EPAUS9rT model with and without scenario. The results are compared with that from AEO 2019 report.

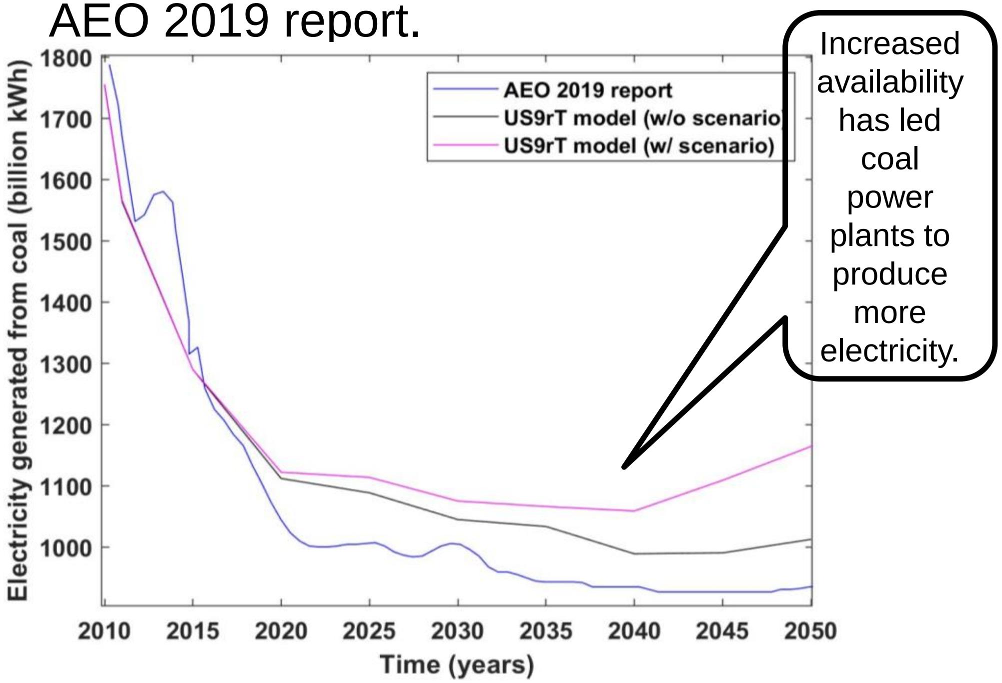

Comparison of amount of electricity generated from coal (billion kWh) from that of the AEO 2019 report, and EPAUS9rT model with and without scenario

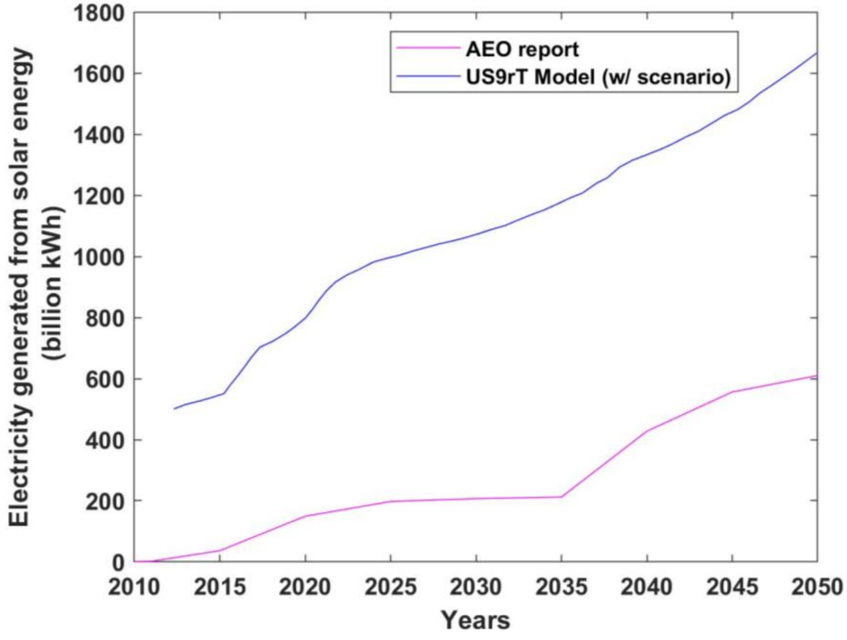

Comparison of amount of electricity generated from solar energy (billion kWh) from that of the AEO 2019 report, and EPAUS9rT model with scenario

Cost-Optimal Sensor Network Synthesis Algorithm

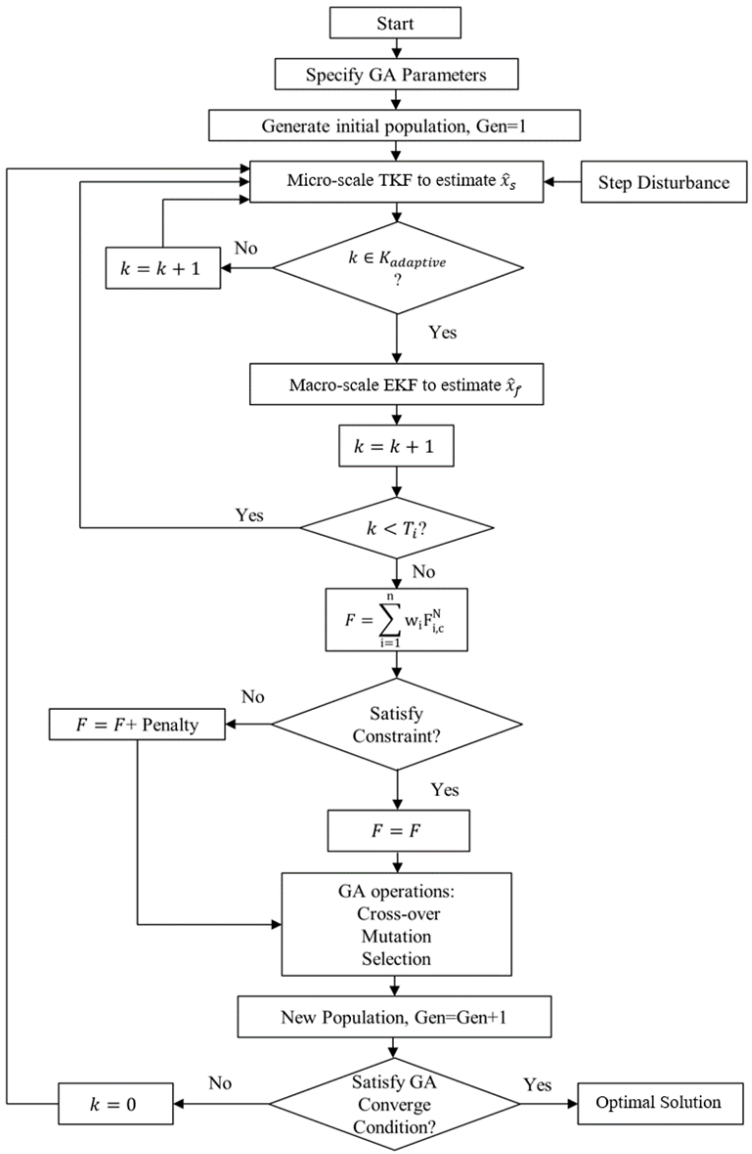

- A cost-Optimal sensor network synthesis algorithm is being developed.
- The objective function takes into account the capital cost of sensors including installation while considering the improvement in plant profitability due to the increased availability because of the installation of the corrosion sensors.
- The integer programming problem is solved by using a genetic algorithm.

SUMMARY & FUTURE WORK

Progress-to-date

- Last sensors has been running @ Longview for seven month with good performance
- Remote data collection has been enabled and data obtained seems to be stable & reasonable
- Real time corrosion monitoring has been realized
- A predictive model has been developed to calculate the corrosion rate by EN data
- Lab-scale RE with good stability and reproducibility has been developed.
- Corrosion database development and techno-economical analysis (TEA) are ongoing in schedule.

Future work

- Incorporate the new RE in the sensor @ Longview.
- Design an anti-dust data acquisition system.
- Continue corrosion database development.
- Continue techno-economical analysis (TEA)
  - using the optimal sensor network
  - Work is also being continued on extracting the projected cost of electricity produced as well from TIMES.

AKNOWLEDGEMENT

DoE-NETL:

- DE-FE 05717: Bob Romanosky, Susan Maley, Chuck Miller, etc.
- DE-FE 31548: John Rockey, Briggs White, Sydni Credle, Jessica Mullen, etc.

Collaborators and Partners:

- WRI - Don Collins, Vijay Sethi
- Special Metals - Jack deBarbadillo, Brian Baker, Gaylord Smith
- ILZRO - Frank Goodwin
- NETL-Albany - Paul Jablonski, Jeff Hawk, Gordon Holcomb, Dave Alman etc.
- Longview Power – Jared Custer, Chad Hufnage, Jeffrey Westfall
- Aspinity - Brandon Rumberg, Don Boucher